Three-Dimensional Structures and Properties of a Transforming and a Nontransforming Glycine-12 Mutant of p21$^{H\text{-}ras}$ †,‡

Sybille M. Franken,§ Axel J. Scheidig, Ute Krengel,‖ Hans Rensland, Alfred Lautwein, Matthias Geyer, Klaus Scheffzek, Roger S. Goody, Hans Robert Kalbitzer, Emil F. Pai,‖ and Alfred Wittinghofer*

Abteilung Biophysik, Max-Planck-Institut für Medizinische Forschung, Jahnstrasse 29, 6900 Heidelberg, Germany

Received December 28, 1992; Revised Manuscript Received April 1, 1993

ABSTRACT: The three-dimensional structures and biochemical properties of two mutants of the G-domain (residues 1–166) of p21$^{H\text{-}ras}$, p21(G12D) and p21(G12P), have been determined in the triphosphate-bound form using guanosine 5′-(β,γ-imido)triphosphate (GppNHp). They correspond to the most frequent oncogenic and the only nononcogenic mutation of Gly-12, respectively. The G12D mutation is the only mutant analyzed so far that crystallizes in a space group different from wild type, and the atomic model of the protein shows the most drastic changes of structure around the active site as compared to wild-type p21. This is due to the interactions of the aspartic acid side chain with Tyr-32, Gln-61, and the γ-phosphate, which result in reduced mobility of these structural elements. The interaction between the carboxylate group of Asp-12 and the γ-phosphate is mediated by a shared proton, which we show by ^{31}P NMR measurements to exist in solution as well. The structure of p21(G12P) is remarkably similar to that of wild-type p21 in the active site, including the position of the nucleophilic water. The pyrrolidine ring of Pro-12 points outward and seems to be responsible for the weaker affinity toward GAP (GTPase-activating protein) and the failure of GAP to stimulate GTP hydrolysis.

The *ras* gene is believed to play an important role in signal transduction via membrane-bound receptor protein kinases. The three mammalian *ras* genes (N-, K-, and H-*ras*) code for a highly conserved guanine nucleotide binding protein with a molecular mass of 21 kDa. The protein functions as a molecular switch which cycles between the GTP-bound active form and the GDP-bound inactive form [for reviews, see Barbacid (1987) and Grand and Owen (1991)]. In the active form it is coupled to a signal transduction cascade that ultimately leads to growth or differentiation. When quiescent fibroblasts are stimulated with EGF or PDGF, p21[1] becomes loaded with GTP and thus is competent to transmit a growth-promoting signal (Satoh et al., 1990a,b). Similarly, activation of T-cells or treatment of PC12 cells with NGF leads to an increase in the fraction of p21 bound to GTP (Downward et al., 1990; Muroya et al., 1992). *Ras* is also considered to be involved in tumorigenesis, since *ras* oncogenes are found in a high percentage of human tumors. If the *ras* protooncogene is found to be activated, it involves in more than 95% of the cases investigated a point mutation in either residue Gly-12 or residue Gln-61. These mutants of p21 are believed to be oncogenic because they are unable to hydrolyze GTP in the presence of GAP, the GTPase-activating protein, which returns p21·GTP to the inactive GDP-bound state by stimulating the intrinsic GTPase activity. The three-dimensional structure of C-terminal truncated forms of p21$^{H\text{-}ras}$ in the GTP-bound state was solved using nonhydrolyzable analogues of GTP (Pai et al., 1989, 1990; Milburn et al., 1990; Privé et al., 1992). This has enabled us to define the interactions between p21 and nucleotide and to suggest a possible mechanism for the GTPase reaction (Pai et al., 1990). Since we have also determined the 3D structure of oncogenic mutants with amino acid substitutions at Gly-12 and Gln-61, we could give a possible explanation at the atomic level why each different mutation is unable to hydrolyze GTP (Krengel et al., 1990). Here we have investigated the properties and the three-dimensional structures of p21$^{H\text{-}ras}$ mutants containing an Asp-12 or a Pro-12 mutation, which we assumed would be the most drastic oncogenic and the most conservative nononcogenic substitution on Gly-12, respectively. This was prompted by the observations by Seeburg et al. (1984) that the replacement of Gly-12 by any other amino acid except proline renders the protein oncogenic and by the assumption that the negatively charged carboxylate side chain of p21(G12D) would disturb the environment of the negatively charged γ-phosphate.

MATERIALS AND METHODS

Cloning Techniques and Mutagenesis. Restriction endonucleases, T4 DNA ligase, polynucleotide kinase, and dNTP's were from Boehringer Mannheim, FRG. The above reagents were used as described in the laboratory manual of Sambrock et al. (1989). Mutant cDNAs for p21 with the G12D and G12P mutations were created by PCR. The forward primers had the sequence 5′-AGGAAACAGAATTCTATGACA-GAATACAAGCTTGTTGTTGTTGGCGCCCCGGTG-TGGGC-3′ for the G12P mutation (the mutated codons and restriction sites are underlined) and 5′-AGGAAACAGAATT-CTATGACAGAATACAAGCTTGTTGTTGTTGGCGC-CGACGGTGTGGGC-3′ for G12D; the reverse primer for both reactions was 5′-CACCAGCACCATGGGCACGTC-3′. A PCR reaction with 30 cycles (30 s at 92 °C, 60 s at 60 °C, 90 s at 72 °C) was done under standard conditions using

† This study was supported by the Stiftung Stipendien-Fonds des Verbandes der Chemischen Industrie (to A.J.S. and U.K.) and NCI Grant SRC 42, Uo1 CA 51992 (to S.M.F. and K.S.).

‡ Crystallographic coordinates have been deposited in the Brookhaven Protein Data Bank under the file names P821P and P1AGP.

* To whom correspondence should be addressed.

§ Current address: Laboratory of Chemical Physics, Faculty of Chemical Technology, University of Twente, 7500 Enschede, The Netherlands.

‖ Current address: Department of Biochemistry and Molecular and Medical Genetics, University of Toronto, Medical Sciences Building, Ontario M5S 1A8, Canada.

[1] Abbreviations: p21, the protein product of the human c-H-*ras* protooncogene; AppNHp, adenosine 5′-(β,γ-imido)triphosphate; GppNHp, guanosine 5′-(β,γ-imido)triphosphate; DTE, dithioerythritol; GAP, GTPase-activating protein; WT, wild-type.

0006-2960/93/0432-8411$04.00/0

150 ng of template DNA, 50 pmol of oligonucleotides, 200 μM dNTP's, and 4 units of Taq polymerase in PCR buffer (Boehringer). Fragments were isolated using Geneclean (Renner GmbH), digested with *Eco*RI and *Nco*I, and ligated into the corresponding fragment from the expression vector ptacrasC′ (John et al., 1988). The sequence of the insert was verified by DNA sequencing using the T7 polymerase kit from Pharmacia. The *Escherichia coli* strain CK600K was used as a host, which is K12 wild-type CK600 containing the plasmid pDMI,1 (Certa et al., 1986) carrying the *lacI*^{q} gene and a kanamycin resistance gene (K). This plasmid is compatible with the expression plasmids described here.

Protein Purification. The biochemical and structural studies were done with mutated, truncated proteins containing amino acids 1–166 (John et al., 1989). The purifications were performed essentially as described previously (Tucker et al., 1986; John et al., 1988). The final purity of the proteins was >95%, as judged from sodium dodecyl sulfate–polyacrylamide gel electrophoresis. Proteins contained 1 mol of guanine nucleotide bound/mol of protein, 85–95% of which could be exchanged against free GDP. Protein concentrations were determined with the Bradford assay using bovine serum albumin as standard (Bradford, 1976), while [8-^{3}H]GDP binding activity was determined by the filter binding assay (Tucker et al., 1986). Standard buffer was, unless stated otherwise, 64 mM Tris-HCl, pH 7.6, 1 mM DTE, 10 mM $MgCl_2$, and 1 mM sodium azide. Exchange of protein-bound nucleotide, usually GDP, was as described by John et al. (1990).

GTPase Activity. (A) Intrinsic. GTPase activity measurements were performed essentially as described previously (John et al., 1989). Briefly, p21·GDP (2 μM) was preincubated with [γ-^{32}P]GTP (40 μM) for 30 min at room temperature in a total volume of 1 mL in 1 mM EDTA, 64 mM Tris-HCl, pH 7.6, 2 mM DTE, and 1 mM sodium azide. The concentration of $MgCl_2$ was then brought to 10 mM, and the temperature was raised to 37 °C. Then 50-μL portions were removed at defined time intervals, and the production of liberated $^{32}P_i$ was measured as described. The experimental errors for GTPase and other rate measurements were between 10% and 20%.

(B) In the Presence of GAP. Complexes between p21 and [γ-^{32}P]GTP were formed by incubating the protein for 5 min with the radioactive nucleotide in the presence of 1 mM EDTA, and 64 mM Tris-HCl, pH 7.6, and 1 mM DTE. Excess nucleotide was removed by gel filtration on a small Sephadex G-25 column (NAP-5, Pharmacia LKB) equilibrated with the GAP reaction buffer: 20 mM Hepes–NaOH, pH 7.6, 1 mM sodium azide, and 1 mM DTE. The protein was eluted from this column with the same buffer. The GTPase reaction was started by addition of 2 mM $MgCl_2$ and the appropriate amount of recombinant human GAP (>2.5 nM). The GTPase reaction was measured as described (Vogel et al., 1988; Frech et al., 1990; Gideon et al., 1992) by following the decrease of the concentration of [γ-^{32}P]GTP bound to p21 by filtration of the reaction mixture through nitrocellulose filters (pore size 0.45 μm). The initial rates were determined from the decrease of p21·GTP concentration with time.

Affinity Constants for p21·GAP Interaction. The affinities of the Gly-12 p21 mutants toward GAP were measured by using p21·GppNHp complexes to inhibit the GAP-mediated GTPase reaction of the fluorescent mutant p21(Y32W). This mutant has been shown to have wild-type properties toward GAP (H. Rensland, unpublished results) and shows a large fluorescent change on GTP hydrolysis. p21(Y32W)·GTP, p21(WT)·GppNHp, p21(G12D)·GppNHp, and p21(G12P)·GppNHp complexes were formed by incubation with excess nucleotide as described (John et al., 1990). Excess nucleotide was removed by gel filtration in reaction buffer: 40 mM Hepes–NaOH, pH 7.6. Concentrations of protein–nucleoside triphosphate complexes were determined by measuring the nucleotide concentration on an HPLC C18 column (Feuerstein et al., 1987). The reaction at 25 °C was started after adding 2 mM $MgCl_2$ and 14 nM GAP expressed in insect cells (Gideon et al., 1992) and followed by monitoring the fluorescence emission at 350 nm (excitation wavelength 297 nm). Varying concentrations of wild-type p21·GppNHp (2–100 μM), which has a dissociation constant K_d of 4.8 μM to GAP (Gideon et al., 1992), were used to determine the K_M of the reaction between p21(Y32W) and GAP as 2.9 ± 0.9 μM. Varying concentrations of mutant p21·GppNHp complexes were used similarly to determine their inhibition constants. The apparent reaction rates were determined from the initial rate of the reaction or by fitting to an exponential curve. (Although this is not mathematically formally correct, the fit obtained was good and could be used to calculate the initial velocity.) The inhibition constants K_i were determined from the apparent reaction rates and have an overall error of 15–30%.

Determination of Melting Temperature by Circular Dichroism. A solution of p21 complexed with GppNHp (0.13 mg/mL) in 10 mM potassium phosphate buffer, pH 7.6, and 2 mM DTE was filled into a quartz fluorescence cuvette with 4-mm light path and 1.8-mL total volume. The circular dichroism was recorded with a Jobin-Yvon Dichrograph mark III at a fixed wavelength of 220 nm. The temperature increase per time was 40 °C/h using a Haake F3 water bath. The temperature was measured directly within the cuvette. The melting temperature was determined by extrapolating the plot of the calculated differences of consecutive values as a function of temperature (Figure 1).

Crystallization. The tightly bound nucleotide GDP was exchanged for the slowly hydrolyzing GTP analogue GppNHp according to John et al. (1990). The mutants were crystallized at room temperature basically following the procedure of Scherer et al. (1989). As precipitant, 25% (w/v) PEG 400 (Serva) in standard buffer solution including 10 mM $MgCl_2$ was used. In the case of the G12D mutant, it was necessary to add 0.07% octyl β-D-glucopyranoside (Sigma). The protein concentration in the droplets was 10 mg/mL. For growing large crystals of the G12P mutant, a microseeding technique according to Schlichting et al. (1989) was used.

Data Collection. X-ray diffraction data were collected at 4 °C on an electronic area detector (Siemens/Nicolet, Madison, WI) using Cu Kα radiation. The X-ray source was a GX-18 rotating anode (Elliott/Enraf Nonius, Delft) with Franks double mirror optics for focusing (Franks, 1955). The anode setting was 35 kV and 50 mA. The intensities were collected in frames of 10 min of oscillation range using two different crystal settings for the G12D mutant and four settings for the G12P mutant. Data were processed by the program XDS (Kabsch, 1988a,b), and the different settings were scaled and merged by the program XSCALE by W. Kabsch. Data collection statistics can be found in Table III.

Solving the 3D Structures. The crystals of the G12P mutant were isomorphous to those of native p21 complexed with GppNHp (Pai et al., 1989). The coordinates of the highly refined structure (Pai et al., 1990) without water molecules were used to calculate an initial map. The omitted pyrrolidine ring of Pro-12 was clearly defined in the first and the final electron density maps. The electron density maps were

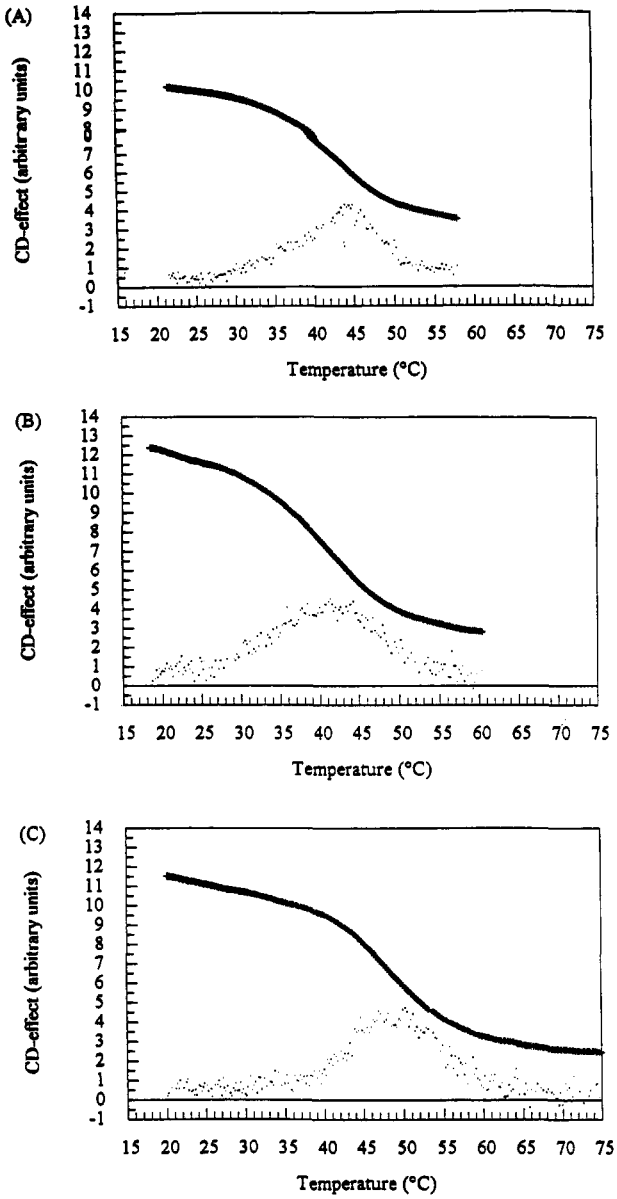

FIGURE 1: Temperature stability of truncated wild-type p21·GppNHp by circular dichroism. The change of ellipticity of a 0.13 mg/mL protein solution in 10 mM phosphate buffer, pH 7.6, and 2 mM DTE was recorded as a function of temperature (×). The apparent melting temperature was determined by extrapolating the plot of the calculated differences of consecutive values as a function of temperature (·). Panels: (A) wild-type p21·GppNHp, (B) p21(G12D)·GppNHp, and (C) p21(G12P)·GppNHp.

calculated with the coefficients $(2mF_o - DF_c)[(\exp(i\alpha_c)]$ to minimize model bias (Read, 1986).

The structure of the G12D mutant was solved by molecular replacement techniques. The search model was the highly refined structure of native truncated p21 (Pai et al., 1990) without nucleotide, Mg^{2+} ion, and water molecules. For the rotational search structure factors were calculated in a *P*1 cell with edge dimensions of 70 Å. All data between 10 and 4 Å were used with a radius of integration of 26 Å. The Fast Rotation function programmed by W. Kabsch following the theory of Crowther (1972) and Tanaka (1977) gave one clear peak at angles of $\alpha = 0°$, $\beta = 179°$ and $\gamma = 151°$. The translation function programmed by W. Kabsch according to Harada et al. (1981) was applied in the resolution range of 10–4 Å and resulted in one sharp peak at $x = 0.167$ and $z = 0.222$ (the origin along y is ambiguous in the monoclinic space group). The initial *R*-factor of the rotated and translated model varied between 35% and 44%, depending on the resolution. Both structures were refined by molecular dynamic methods using the program XPLOR (Brünger et al., 1987). The starting models included protein atoms only with a Gly residue at position 12. After one round of simulated annealing (SA) refinement the models were inspected and rebuilt where necessary. In the case of G12P the pyrrolidine ring was included after the first SA round. After the second round of refinement of the G12D mutant the mutated residue, the nucleotide molecule, and the Mg^{2+} ion were built into the corresponding density, and rebuilding was done manually where necessary.

The interactive work was done using the program FRODO (Jones, 1978) adapted to an Iris 4GT (Silicon Graphics, Mountain View, CA) by Cambillau (1989). After further refinement, solvent molecules were located in difference Fourier and omit maps, respectively, and included in the refinement. For both structures individual isotropic restrained temperature (*B*) factors were refined as soon as the complete structure was very well defined. A summary of the refinement statistics is given in Table IV.

NMR Spectroscopy. The ^{31}P NMR spectra were recorded with a Bruker AMX-500 NMR spectrometer operating at 202 MHz. The spectra were referenced to 85% phosphoric acid contained in a glass capillary which was immersed in the sample. The 2.5-mL samples were contained in 10-mm tubes (Wilmad). Spectra were recorded at 10 °C. The pH values in the samples were varied by addition of appropriate quantities of DCl or NaOD solutions and measured with a combination glass electrode (Ingold). No correction for the isotope effect was made. The titration curves were fitted with the modified Henderson–Hasselbalch equation [see, e.g., Hausser and Kalbitzer (1991)]. The NMR samples contained approximately 1 mM protein [p21·GppNHp·Mg^{2+} or p21(G12D)·GppNHp·Mg^{2+}] in 10 mM Tris-HCl, 2 mM $MgCl_2$, 0.1 mM DTE, and 0.1 mM sodium azide in D_2O. The nucleotide samples contained approximately 10 mM nucleotide (GTP or GppNHp) in the same buffer but with no or 20 mM $MgCl_2$ in the solution.

RESULTS

Biochemical Properties of p21(G12P) and p21(G12D). The two mutants of p21$^{H\text{-}ras}$, in the truncated form containing amino acids 1–166, were created by PCR using corresponding oligonucleotides (see Materials and Methods). The resulting *Eco*RI–*Nco*I fragments were cloned into the ptacrasC′ expression system, expressed in *Escherichia coli*, and purified using the standard two-column procedure (Tucker et al., 1986; John et al., 1989). They will be called p21(G12P) and p21(G12D) henceforth. The biochemical properties of the proteins were determined and are summarized in Table I. As with p21(G12V) and p21(G12R) described earlier (John et al., 1988; Krengel et al., 1990), both mutations decrease slightly the dissociation rate constants for GDP. With GTP there is a drastic increase of the dissociation rate constant for p21(G12D) and only a slight increase with p21(G12P). It has been reported that p21(G12P) has an intrinsic GTPase which is 2.7-fold higher than that of cellular p21. Its intrinsic GTPase could not be stimulated by GAP (Gibbs et al., 1988). We also find the intrinsic GTPase to be higher, albeit to a smaller degree. Using a GTPase assay with fluorescent mantGTP (Neal et al., 1990; Rensland et al., 1991), we find the intrinsic GTPase of p21(G12P) to be similar to that of wild-type p21. Stimulation by GAP (p120-GAP) is very weak. Only with very high concentrations of GAP did we find a

Table I: Biochemical Properties of the Mutant G12D and G12P and Wild-Type p21$^{H\text{-}ras}$ Proteins[a]

protein	WT	G12P	G12D
k_{off}, mGDP, 37 °C ($\times 10^4$ s^{-1})	2	1.4	1.5
k_{off}, mdGDP, 37 °C ($\times 10^4$ s^{-1})	1.1	0.6	0.8
k_{off}, mGppNHp, 37 °C ($\times 10^4$ s^{-1})	11	13	89
k_{GTPase}, [^{32}P]GTP (min^{-1})	0.028	0.043	0.001
k_{GTPase}, mGTP (min^{-1})	0.025	0.027	0.005
GAP stimulation	+++	+	–
K_A(rel),[b] p21·GppNHp·GAP	1	0.3	1[c]

[a] k_{off} and k_{GTPase} are the dissociation and the GTP hydrolysis rate constants; k_{off} was measured with fluorescent mant (m) nucleotides in the spectrofluorometer as described by John et al. (1990) and Rensland et al. (1991); k_{GTPase}, [^{32}P]GTP, was measured with radioactive GTP as described in Materials and Methods. Values for the mutants G12D and G12P were determined for the truncated (residues 1–166) protein. [b] The affinity between wild-type protein and GAP, measured by inhibiting the GAP-stimulated fluorescence increase of p21(Y32W)·GTP, as described in Materials and Methods, was arbitrarily chosen as 1. [c] Determined for p21$^{N\text{-}ras}$ by Bollag and McCormick (1991).

5-fold stimulation of the GTPase reaction. As expected, the p21(G12D) protein has a 4.5-fold reduced GTPase which cannot be stimulated even by high concentrations of GAP, as has been noted before for the corresponding mutant of p21$^{N\text{-}ras}$ (Trahey & McCormick, 1987; Bollag & McCormick, 1991). The affinity of the G12P mutant for GAP (relative to wild type) has been determined using the fluorescent mutant p21(Y32W) that has been shown to be very useful for measuring biochemical properties of p21 (H. Rensland, unpublished results; see Materials and Methods). The affinity is 3.3 times lower than that of normal p21 (Table I), whereas the Asp-12 protein has been reported to have wild-type affinity (Bollag & McCormick, 1991).

It is well-known that single amino acid substitutions in a protein may cause entropic stabilization or destabilization through a reduction or increase in the conformational freedom of the polypeptide chain (Matthews, 1987; Matthews et al., 1987; Alber, 1989; Shortle, 1989). Although the effect on protein thermostability is in general quite small, it depends on the nature of the amino acid and the environment in which it occurs. As proline has less backbone configurational entropy in the denatured state than any other amino acid, it requires less free energy to fold. Since glycine has the highest configurational entropy in the denatured state, the substitution of glycine by proline should decrease the configurational entropy of unfolding of the polypeptide backbone and thus stabilize the protein.

To test this, we measured the temperature of unfolding for wild-type and mutant (truncated) proteins complexed to GppNHp. The loss of defined 3D structure which accompanies denaturation was monitored spectroscopically following the temperature dependence of the circular dichroism (CD) signal at 220 nm for the wild-type and mutant protein. The truncated p21 proteins could not be refolded after the solution was heated to 65 °C, as evidenced by the irreversible nature of the melting curve. This is in contrast to the behavior of the full-length protein, which can be reversibly heat-denatured (Reinstein et al., 1991; P. Gideon, unpublished results). The resulting apparent melting temperature of truncated p21(1–166) is 44 °C and thus is 11 deg lower than the melting temperature of full-length protein (Reinstein et al., 1991). The C-terminal deletion of p21 does not change the interactions of the protein with guanine nucleotide, GAP, or guanine nucleotide-releasing protein, as reported (John et al., 1989; Mistou et al., 1992; Gideon et al., 1992). It does, however, dramatically alter the thermal stability. As predicted, the G12P mutant increases the thermal stability of p21, in this case by 5 °C, whereas the G12D mutation has no significant effect (Figure 1 and Table II).

Table II: Melting Temperatures of Truncated Wild-Type and Mutant p21$^{H\text{-}ras}$ Determined Using CD Spectroscopy at 220 nm

protein	T_m (°C)
wild-type p21	44 ± 1
G12D mutant	42 ± 1
G12P mutant	49 ± 1

Table III: Crystallographic Data and Statistics of Data Collection

	G12D	G12P
space group	$C2$	$P3_221$
unit cell parameters	a = 69.9 Å	$a = b$ = 40.2 Å
	b = 39.8 Å	c = 160.1 Å
	c = 56.1 Å	
	$\alpha = \gamma$ = 90°	$\alpha = \beta$ = 90°
	β = 107.4°	γ = 120°
V_M (Å^3/Da)	2.0	1.9
molecules per asymmetric unit	1	1
crystal size (mm × mm × mm)	0.3 × 0.3 × 0.15	1.1 × 0.3 × 0.15
max resolution (Å)	2.2	1.4
no. of obsd reflections	10 475	102 376
no. of unique reflections (completeness)		
$F_o > 0\sigma$	5 195 (59.2%)	25 400 (82.7%)
$F_o > 1\sigma$	5 068 (57.8%)	22 324 (72.7%)
$F_o > 2\sigma$	4 924 (56.1%)	18 209 (59.3%)
R_{merge}[a] (%), $F_o > 0\sigma$	4.7	8.8

[a] $R_{merge} = \sum_{hkl}\sum_i|I_{i,hkl} + \langle I_{hkl}\rangle|/\sum_{hkl}\langle I_{hkl}\rangle$, where $I_{i,hkl}$ and $\langle I_{hkl}\rangle$ are the intensity values of individual measurements and of the corresponding mean values; the summation is over all measurements.

Table IV: Refinement Results of the Final Models

	G12D	G12P
resolution range for refinement (Å)	8.0–2.3	6.0–1.5
no. of amino acids	166	166
no. of water molecules	38	118
no. of non-hydrogen atoms		
all	1397	1476
protein	1326	1325
nucleotide (includes 1 Mg^{2+} ion)	33	33
R-factor[a] (number of used reflections and completeness at above resolution)		
$F_o > 0\sigma$	17.7% (4 656; 70.2%)	22.0% (21 138; 85.9%)
$F_o > 1\sigma$	17.1% (4 522; 68.2%)	20.7% (19 577; 79.5%)
$F_o > 2\sigma$	16.6% (4 294; 64.8%)	19.8% (16 898; 68.7%)
R-factor without water		
$F_o > 1\sigma$	20.2%	24.7%
av temperature factor (Å^2)		
all non-hydrogen protein atoms	12.54	20.05
water molecules	26.62	38.41
rms deviations from ideal geometry		
bond lengths (Å)	0.016	0.015
bond angles (deg)	3.2	2.8
estd coordinate error (Å)		
from σ_A plot (Read, 1986)	0.22	0.20

[a] R-factor = $(\sum|F_o - F_c|)/(\sum|F_o|)$.

Crystallization and X-ray Structure. Tables III and IV show the crystallographic data and the refinement statistics for the two mutants. The G12D mutant is so far the only mutant of truncated p21(1–166) complexed with GppNHp which does not crystallize isomorphously with the native enzyme, but instead in the monoclinic space group $C2$. The highest resolution obtained for the p21(G12D) crystals (2.17

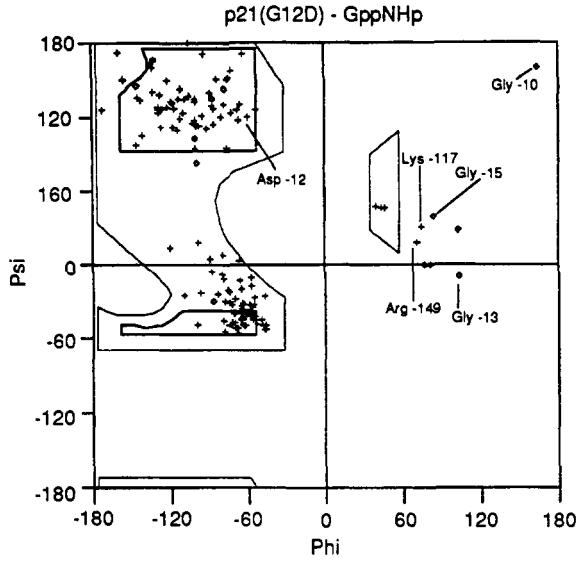

FIGURE 2: Ramachandran plot of the present p21(G12D)·GppNHp model: (+) every residue except glycine; (◇) glycine residues.

Å) is also much lower than for either wild type (1.35 Å) (Pai et al., 1990) or the G12P mutant presented here (1.4 Å). The Ramachandran plot (Figure 2) of the dihedral angles shows that only Lys-117 and Arg-149 of the non-glycine residues have conformations of the polypeptide chain in an unallowed region (Ramachandran et al., 1963). It is gratifying that these residues and the glycine residues shown have the same conformational angles as observed in the wild-type structure crystallizing in a trigonal space group ($P3_221$), suggesting that these conformational angles are not due to crystal packing forces.

The structures of wild-type and mutant (G12D) p21 are very similar. The overall root-mean-square (rms) deviation of all C_α atoms is 0.54 Å; leaving out loop L4 (residues 60–70) reduces it to 0.28 Å. With all side chains included in the calculations, the deviations are 1.14 and 0.89 Å, respectively. However, G12D crystallizes in a space group different from that of the wild-type protein; the Ramachandran plot (Figure 2) indicates the same residues outside the preferred regions as in the wild-type structure (Pai et al., 1990). Therefore, the conformations of these residues should mainly not be affected by the crystal packing interactions. A plot of the rms deviations per residue (Figure 3) shows that the residues in loop L4 (especially residues 62–67) have the highest deviation from the native structure. This has been found in other mutant structures as well (Krengel et al., 1990). In most of those structures the electron density for these residues was poorly defined, and often several conformations of residues 61–65 could be defined. In the G12D mutant the density in this region is well-defined, and residues 62–67 form a 3_{10} helix, as analyzed by the program DSSP (Kabsch & Sander, 1983), and there is no indication of any alternative conformations. In the native structure the 3_{10} helix only starts at residue 65, and residues 62 and 63 belong to a turn and residue 64 belongs to a bend. The more rigid conformation in the mutant structure is also reflected by the temperature factors of the atoms in this region. The average temperature factor for residues 61–67 is 23.9 Å^2 in the mutant structure (compared to 13.4 Å^2 for the rest of the molecule) whereas it is 49.9 Å^2 in the case of the native structure (17.3 Å^2 for the rest of the protein) [see Figure 4 of Pai et al. (1990)].

One of the reasons for the well-defined conformations of residues 62–67 appears to be the hydrogen bond between the

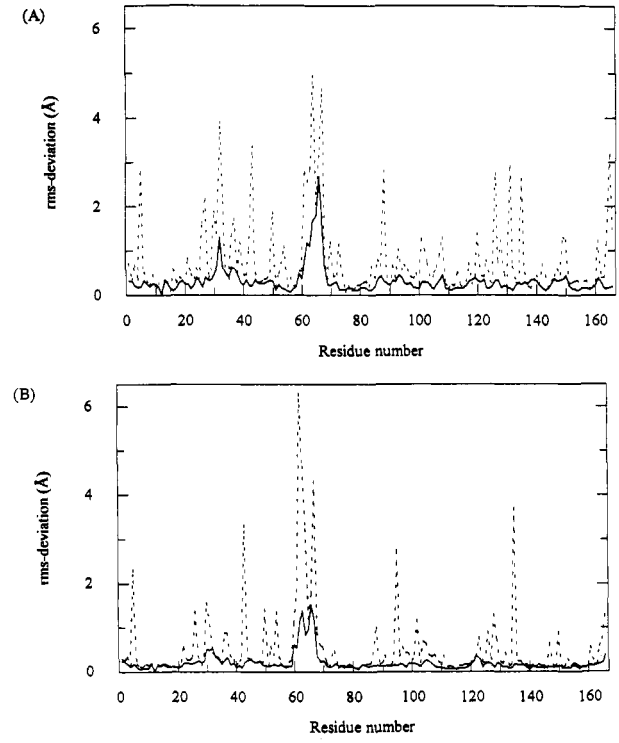

FIGURE 3: Variation of the root-mean-square (rms) deviation against the wild-type structure (Pai et al., 1990) of the main chain (solid line) and side chain (broken line) with the residue number of (A) p21(G12D)·GppNHp and (B) p21(G12P)·GppNHp, respectively.

side chains of Gln-61 and Asp-12 [NE2(61)–OD1(12), 3.14 Å] shown in Figure 4 which fixes the start of the helix. The second obvious deviation from the native structure is residue Tyr-32, whose rms deviation of the main-chain atoms is 1.3 Å and of the side-chain atoms 3.9 Å. This change of position of Tyr-32 appears to be due to a hydrogen bond between the terminal OH group of the tyrosine ring and the side chain of Asp-12 [O(32)–OD2(12), 2.7 Å] (Figure 4). Whereas in all the other Gly-12 mutants the Tyr-32 side chain takes up roughly the same orientation, it appears to be pulled more toward the interior of the protein in p21(G12D). In general, Tyr-32 is very flexible and may exhibit different conformations as could be shown in crystal structures of p21 complexed with different GTP analogues (A. Scheidig, unpublished results). As there are no limiting packing forces or contact surface areas between the Tyr-32 side chain and the nucleotide or the neighboring protein molecule in the crystal of p21(G12D)·GppNHp, the hydrogen bond between Tyr-32 and Asp-12 is apparently the driving force for the structural rearrangement. Due to this new orientation in the G12D structure, Tyr-32 also does not bind to the γ-phosphate oxygen of the neighboring molecule as in other structures (Krengel et al., 1990; Pai et al., 1990).

The position of the bound Mg^{2+}·nucleotide complex in p21(G12D) is similar to that in the native structure (rms deviation 0.2 Å), but it is in a somewhat different environment. In contrast to the octahedral coordination of the Mg^{2+} ion in the native and G12P structures, only five ligands are found in the G12D mutant structure, with one of the water ligands (Wat-173) missing. Mg^{2+} is shifted 1.2 Å in a direction away from the nucleotide, and the ligands OG of Ser-17 and OG1 of Thr-35 are shifted toward the previous Wat-173 position (see Figure 5). The environment of the γ-phosphate is different in that water molecules corresponding to Wat-175 and Wat-189, which are bound to an oxygen of the γ-phosphate group in the native structure, cannot be found in the mutant structure.

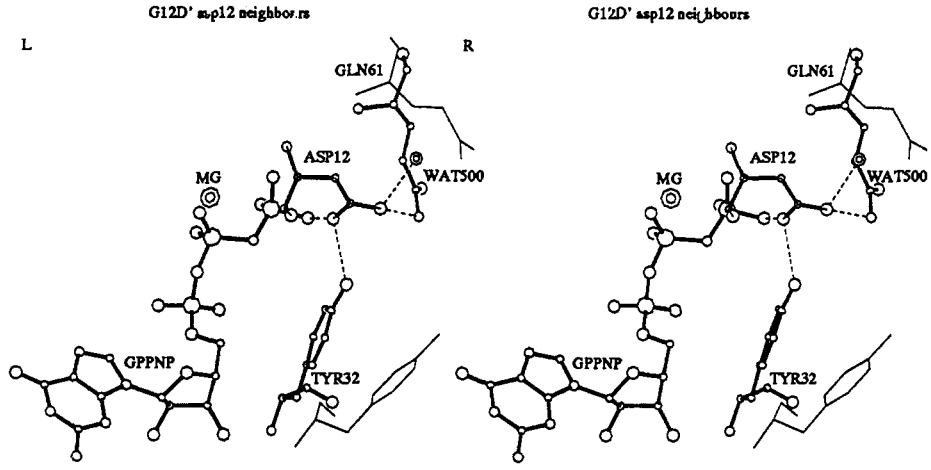

FIGURE 4: Stereo plot of the Asp-12 residue and its neighbors in the G12D mutant structure (thick lines) compared with the native structure (thin lines). Dashed lines indicate hydrogen bonds with the following distances: OD1(Asp-12)–OH2(Wat-500), 2.8 Å; OD1(Asp-12)···NE2(Gln-61), 3.1 Å; OD2(Asp-12)···O1PC(GppNHp), 2.7 Å; OD2(Asp-12)···OH(Tyr-32), 2.7 Å.

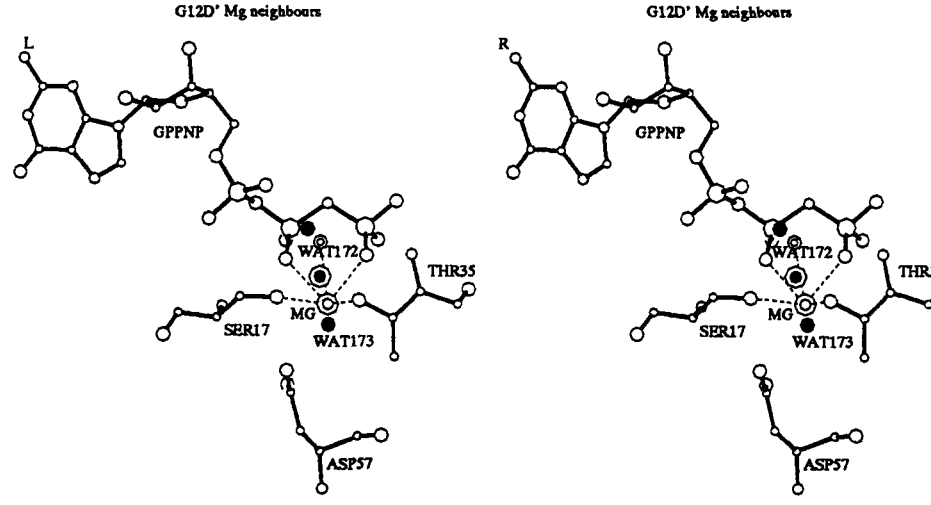

FIGURE 5: Stereo plot of the coordination of the Mg^{2+} ion in the G12D mutant and the native structure. Dashed lines indicate the distances to the closest ligands: Mg···OG(Ser-17), 2.6 Å; Mg···OG1(Thr-35), 2.6 Å; Mg···O2PB, 2.4 Å; Mg···O2PC, 2.4 Å; Mg···OH2(Wat-172), 2.7 Å. OD1 and OD2 of Asp-57 are both 3.4 Å away from the Mg^{2+} ion. The positions of magnesium and water ligands of the native structure deviating from (Wat-172, MG) or missing in (Wat-173) the G12D mutant structure are indicated by black circles.

The water molecule Wat-175 is believed to be the nucleophile involved in GTP hydrolysis. A superposition of the native and the G12D structures including the waters reveals that there would be enough room for Wat-175, but no density can be found. Probably a corresponding nucleophilic water is not as tightly bound in the crystal structure of p21(G12D) as in the wild-type structure.

Except for these two obvious changes, the presence of the aspartate side chain does not perturb the native conformation. OD2 of Asp-12 is only 2.65 Å away from one of the oxygens of the γ-phosphate of GppNHp. In the omit map density and in the initial density after molecular replacement, calculated without the Asp-12 side chain, the orientation of the carboxylate side chain is clearly defined (Figure 6). The potential energy of the interaction of OD2 with its environment (calculated with XPLOR; Brünger et al., 1987) would be around 3 kcal/mol, assuming a negative charge on the γ-phosphate oxygen and on the carboxylate side chain. This energy is higher than that of any other Asp side chain in the protein. Protonating the γ-phosphate as suggested by the ^{31}P NMR spectroscopic experiments (see below) would lower the energy of OD2 to −9.6 kcal/mol, which is in the range of energies found at other carboxyl groups in the structure of p21.

The terminal phosphate of AppNHp has been found to be about a 10-fold weaker acid than ATP (pK_a = 7.7–7.9 vs pK_a = 7) (Yount, 1975). Assuming that GppNHp has a similar pK_a relative to GTP (pK_a = 6.7; Rösch et al., 1980) and assuming also that, as usual, the pK_a value for the terminal phosphate is further reduced due to the coordination to Mg^{2+}, it seemed unlikely that the terminal phosphate could be protonated in either wild-type or mutant p21 at the pH of 7.4 of the mother liquor. As described below, for this reason we determined the pK_a value of GppNHp free in solution, complexed to Mg^{2+}, and bound to p21 by using ^{31}P NMR spectroscopy.

As described for a number of other p21 mutants (Krengel et al., 1990), p21(G12P) crystallizes isomorphously to native p21 (space group $P3_221$). The refined crystal structure of this mutant converged at a crystallographic R-factor of 22.02% for 21 138 unique reflections between 6.0- and 1.5-Å resolution. The root-mean-square deviations from ideality in bond lengths and in bond angles are 0.015 Å and 2.8°, respectively, which is in a reasonable range for a small protein at this resolution. In the final electron density map nearly every atom is well-defined by density, with the exception of residues 62, 63, and 66. The electron density of residue 61 is good but reflects

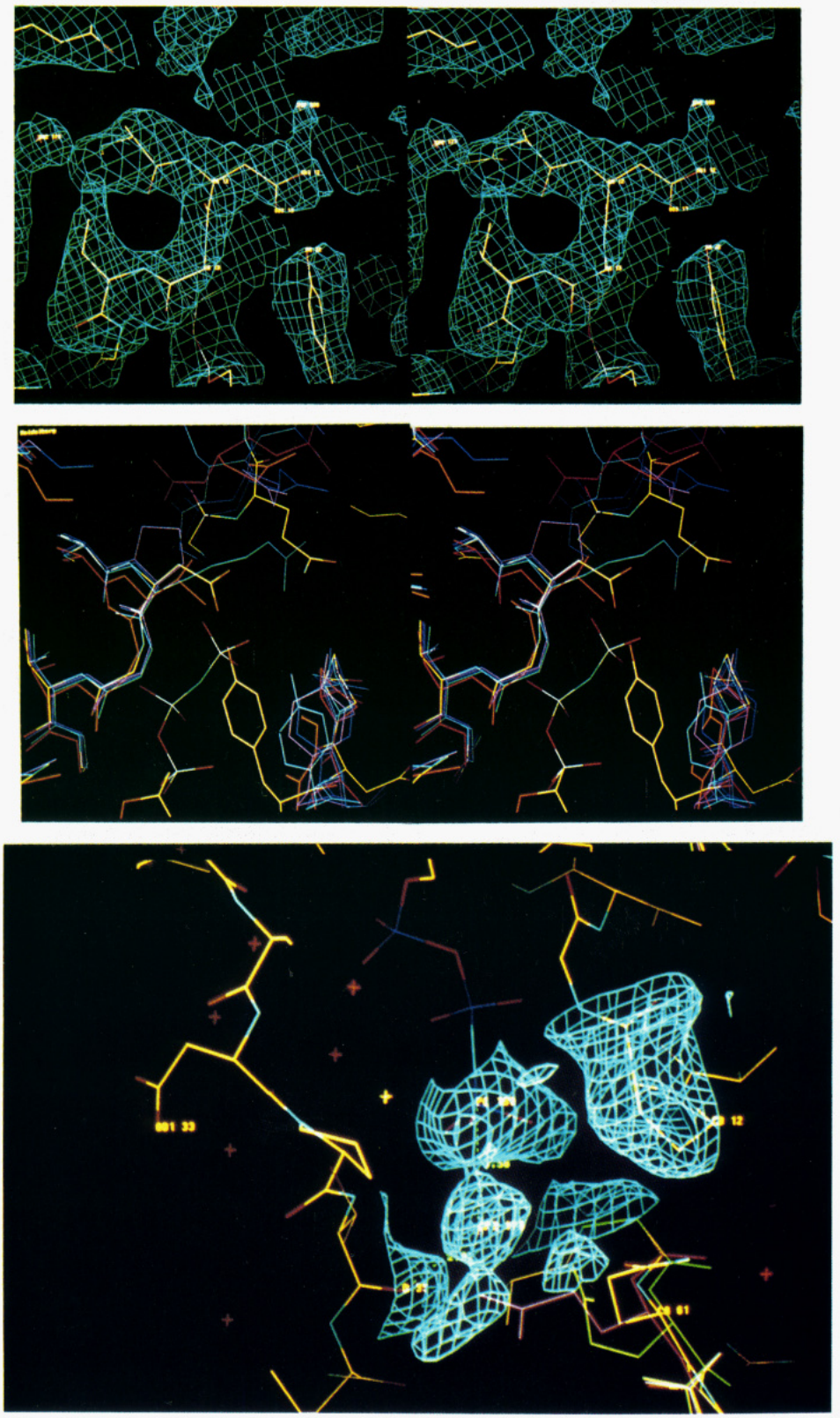

FIGURE 6: (A, top) Stereoview of the original omit (without Asp-12) electron density map of p21(G12D) around the omitted Asp-12 side chain (15% cutoff of the maximum). The starting model for the simulated annealing refinement contained only Gly at this position. (B, middle) Stereoview of an overlay of various mutant Gly-12 structures in the triphosphate conformation around the active site. The model for p21(G12D) is multicolored; the unicolored models are as follows: p21(G12P), magenta (this paper); p21(G12V), red (Krengel et al., 1990); p21(G12R), blue (Krengel et al., 1990). (C, bottom) Part of the final omit (without Pro-12) electron density map of p21(G12P) around the water molecule Wat-175 (7% cutoff from the maximum). The nucleotide is shown with a van der Waals sphere. The possible catalytically active conformations of Gln-61 are indicated in green and red, respectively.

more than one possible conformation (Figure 6). This is also reflected in the high temperature factor of 49.5 Å^2 for all atoms of residues 61–67, compared to the mean value of 20.1 Å^2 for the other residues. This observation has been found for wild-type p21 (Pai et al., 1990) and other mutants of p21 (Krengel et al., 1990) as well.

In Figure 6 an example of the electron density map shows the location of the extra pyrrolidine ring of the Pro-12 mutant.

Table V: Chemical Shifts and pK_a Values of the α-, β-, and γ-Phosphate of GTP and GppNHp and Complexes of GppNHp with p21 Proteins[a]

molecule	group	pK_a	δ_{AH}/ppm	δ_{A^-}/ppm
GppNHp	α	9.0 ± 0.3	−10.25 ± 0.04	−9.81 ± 0.06
	β	8.7 ± 0.1	−10.3 ± 0.1	−6.7 ± 0.1
	γ	8.9 ± 0.2	−1.09 ± 0.6	0.08 ± 0.06
GTP	α	6.3 ± 0.2	−10.67 ± 0.02	−10.40 ± 0.02
	β	6.3 ± 0.1	−22.37 ± 0.03	−20.88 ± 0.03
	γ	6.3 ± 0.1	−10.07 ± 0.05	−5.17 ± 0.04
GppNHp·Mg^{2+}	α	6.5 ± 0.3	−9.78 ± 0.05	−9.48 ± 0.04
	β	6.3 ± 0.1	−8.5 ± 0.1	−4.9 ± 0.1
	γ	6.3 ± 0.2	−1.72 ± 0.08	−0.46 ± 0.06
GTP·Mg^{2+}	α	4.8 ± 0.1	−10.67 ± 0.02	−10.07 ± 0.07
	β	4.7 ± 0.1	−21.56 ± 0.05	−18.66 ± 0.03
	γ	4.7 ± 0.1	−9.94 ± 0.06	−4.96 ± 0.03
p21(WT)·GppNHp·Mg^{2+}	α	5.4 ± 0.9	−11.24 ± 0.09	−11.05 ± 0.03
	β	6.2 ± 0.8	−2.09 ± 0.05	−2.39 ± 0.01
	γ	5.1 ± 0.3	−0.26 ± 0.09	0.40 ± 0.02
p21(G12D)·GppNHp·Mg^{2+}	α	7.0 ± 0.3	−11.33 ± 0.03	−10.98 ± 0.06
	β	6.7 ± 0.1	−0.47 ± 0.09	−2.75 ± 0.09
	γ	6.5 ± 0.3	−3.1 ± 0.2	0.3 ± 0.2

[a] δ_{AH} and δ_{A^-} are fit parameters describing the chemical shifts of the 3-fold and 4-fold negatively charged nucleotide, respectively. The errors given correspond to 95% confidence levels; the different samples were recorded under identical experimental conditions (see Materials and Methods).

The rms deviation of atomic coordinates for the main-chain and side-chain non-hydrogen protein and nucleotide atoms between wild-type and G12P protein along the polypeptide chain is shown in Figure 3. In both structures the water molecule Wat-175 is very well defined, which is proposed as the activated water molecule (Pai et al., 1990). The average value over the entire protein is 0.1948 and 0.5240 Å, respectively. This value and a direct superposition indicated that these two structures are nearly identical, making G12P the most conservative substitution of p21 analyzed structurally so far. Since no difference in the crystal structure and the diffraction power could be determined, and since the crystals of p21(G12P) exhibit significantly less mosaic spread, they are now used regularly for Laue X-ray diffraction studies (Scheidig et al., 1992).

^{31}P NMR Spectroscopy. To determine whether the proton presumably shared between the γ-phosphate and the carboxylate side chain of Asp-12 could also be identified in solution, we examined the ^{31}P NMR spectra of GppNHp complexed to wild-type p21 and the Asp-12 mutant. As a control we show in Table V that GppNHp free in solution has a pK_a of 8.7 for the dissociation of the second proton of the γ-phosphate, which is approximately 2.4 pH units higher than for GTP measured under identical experimental conditions. This means that the three phosphates of GTP carry four negative charges and those of GppNHp only three at physiological pH (see Table V). A similar shift in pK_a has been reported for AppNHp as compared to ATP (Yount, 1975). As expected, the pK_a decreases dramatically when Mg^{2+} is complexed to the nucleotide (see Table V). It is remarkable that for GppNHp, but not for GTP, the second deprotonation of the γ-phosphate produces a much larger shift on the β-phosphate than on the γ-phosphate. This has also been noticed for ATP and AppNHp (Tran-Dinh & Roux, 1977). Figure 7 shows the pH dependence of chemical shifts of the phosphate groups of GppNHp·Mg^{2+} complexed to wild-type p21. Compared to free GppNHp·Mg^{2+} the chemical shifts of all phosphate groups change after binding to the protein. For the completely deprotonated form (A^-) of the

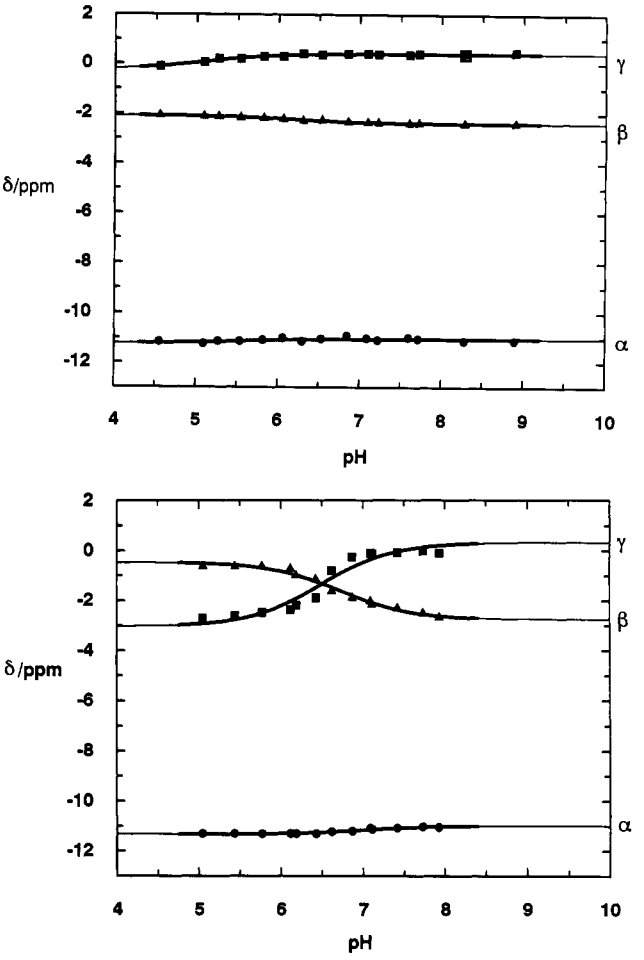

FIGURE 7: pH dependence of ^{31}P NMR chemical shifts for the phosphate residues of GppNHp·Mg^{2+} complexed with wild-type (A, top) and mutant p21 (B, bottom): 1 mM p21·GppNHp·Mg^{2+} (A) or p21(G21D)·GppNHp·Mg^{2+} (B) in 10 mM Tris-HCl, 2 mM $MgCl_2$, 0.1 mM DTE, and 0.1 mM NaN_3 in D_2O at 10 °C. The ^{31}P NMR shifts of the α-, β-, and γ-phosphate groups of GppNHp are plotted as a function of the pH. Solid lines were calculated with the parameters given in Table V.

nucleotide more changes in chemical shifts on binding of GppNHp to the protein are found for the α- and β-phosphate groups than for the γ-phosphate [compare GppNHp·Mg^{2+} and p21(WT)·GppNHp·Mg^{2+} columns in Table V].

The calculated pK_a values for the second deprotonation of the terminal phosphate of GppNHp·Mg^{2+} and its complexes with p21 vary somewhat when analyzed for the different phosphate groups; however, the fit errors are rather large because of the small pH dependence of chemical shifts. Within the limits of errors, they are more or less identical, as they should be if the pH dependence of chemical shifts reflects solely the protonation–deprotonation of the terminal phosphate groups. [An exception is the β-phosphate group in the p21·GppNHp·Mg^{2+} complex (Table V) where the pK_a obtained has a large error. Since this large error is due to a barely resolved splitting and broadening of the β-phosphate resonance lines, it has been omitted in the calculation of an average pK_a value.] The pK_a values calculated with the assumption mentioned above are then 6.3, 5.2, and 6.7 for free GppNHp·Mg^{2+} and GppNHp·Mg^{2+} bound to wild-type p21 and p21(G12D), respectively.

In the wild-type protein the pK_a of the terminal phosphate group is lower than in the free nucleotide. This could be due to Mg^{2+} being more tightly bound to the nucleotide in the ternary protein–nucleotide–Mg^{2+} complex [$K_D \sim 20$ nM; see

John et al., (1993)] and also due to interactions between the γ-phosphate and the protein which together stabilize the deprotonated state. In the mutant p21(G12D) the protonation of the terminal group is favored. Since the pK_a is likely to be higher in water than in the D_2O used for the NMR measurements, it can be assumed that in solution at neutral pH the terminal phosphate group is sharing a proton with the carboxylate side chain of Asp-12, as found in the crystal structure.

The chemical shifts δ_{AH} and δ_{A^-} of the α-phosphate are identical for the wild-type protein and the mutant p21(G12D) within the limits of error. This means that the environment of this group is, from the NMR point of view, independent of the ionization state of the terminal phosphate. In contrast, the chemical shifts of the β- and γ-phosphate are quite different in the two proteins when the nucleotide is not fully deprotonated. At higher pH values the chemical shifts are again very similar for mutant and wild-type protein. This means that at higher pH values, after deprotonation of the terminal phosphate group, the nucleotide in the mutant protein "sees" an environment similar to that in the wild-type protein. Most probably, the interaction of the aspartyl side chain with the two negative charges of the γ-phosphate leads to a rearrangement of the local structure which removes the aspartyl residue from the vicinity of the γ-phosphate.

The NMR data also show that the Asp-12 mutant is unstable at lower pH values, since the ^{31}P NMR spectrum changes with time and new resonances for the β- and γ-phosphate appear, whereas the intensities of the original resonances decrease concomitantly in intensity (data not shown). The chemical shifts of the new resonances are very close to the wild-type shifts at low pH, indicating a slow, irreversible conformational change of the mutant protein toward a wild-type-like structure.

DISCUSSION

We have analyzed here the three-dimensional structures of two Gly-12 mutants of p21$^{H\text{-}ras}$, which have opposite biological activities. The G12D mutation is one of the most frequent oncogenic mutations of p21 found in the K-*ras* gene in human tumors (Bos et al., 1987; Anderson et al., 1992). The G12P mutation has been generated in vitro and found by DNA transfection studies to be the only mutation of Gly-12 which is nontransforming (Seeburg et al., 1984). We find the GTPase of p21(G12P) to be similar to that of wild-type, whereas that of the G12D mutation is reduced. Both proteins have the common property that their GTPase is not (G12D) or is only very slightly (G12P) stimulated by GAP. Both proteins still bind to GAP, G12D with almost wild-type affinity (Bollag & McCormick, 1991), whereas p21(G12P) has a 3.4-fold lower affinity (Table I).

The three-dimensional structure of p21(G12P) is very similar to that of wild-type p21. Most importantly, the structure analysis shows the existence of a water molecule that is in a position to attack the γ-phosphate for phosphoryl transfer. We can also find a conformation for Gln-61, which we call the catalytic conformation, which puts its side chain into a position to activate this water molecule for nucleophilic attack (Figure 6). This would explain why the intrinsic GTPase of p21(G12P) is unchanged as compared to wild type.

In contrast, we do not find a corresponding water molecule in the G12D protein even though there is enough space for such a water molecule, as could be shown by model building. This can possibly be explained by the fact that Gln-61 is not able to hydrogen bond the water molecule as in the catalytic conformation since it itself makes a hydrogen bond to Asp-12. This water molecule would therefore have only a limited lifetime in the catalytically relevant position because it is not as tightly bound as in the wild-type protein and in the G12P mutant. The absence of the water molecule could, however, also be due to the lower resolution of the p21(G12D) structure.

It is likely that in the p21(G12D)·GTP complex the γ-phosphate is not protonated at physiological pH as found for the corresponding GppNHp complex since Table V shows that the pK_a of the γ-phosphate of GTP is approximately 2 pH units lower than of GppNHp. It is possible that the lower GTPase activity of the Asp-12 mutant is due to the interaction of Asp-12 and Gln-61 side chains which could be retained in the GTP complex. The fact that p21(G12D) cannot be stimulated by GAP is in line with all the evidence for other oncogenic p21 proteins: all the mutants whose intrinsic GTPase is reduced also cannot or, as in the case of p21(Q61H) (Bollag & McCormick, 1991), can only partially be stimulated by GAP. Under physiological conditions the GTPase of p21(G12P) is not stimulated by GAP and reacts normally with the nucleotide-releasing protein (Mistou et al., 1992). Because the protein is therefore most likely in the GTP-bound conformation in vivo, it is more difficult to explain why this mutant would not be transforming. Figure 6 shows the active site of mutant G12P protein as seen from the viewpoint of an effector molecule: the pyrrolidine ring of the mutant projects into the solvent and could thus possibly prevent the close contact with an incoming effector molecule. This could either be GAP, if GAP alone is the signal terminator and signal effector (McCormick, 1989), or be a complex of GAP with another as yet unknown molecule being the signal transmitter (Bourne & Stryer, 1992). Since we have found that the affinity of GAP for the nononcogenic p21(G12P) is reduced only 3.4-fold, whereas oncogenic Gly-12 mutants such as p21(G12V) and p21(G12R) have much lower affinities for GAP (Vogel et al., 1988; Gideon et al., 1992), our results would favor the idea that GAP is not the sole effector molecule.

ACKNOWLEDGMENT

We thank Alfred Pingoud for help with the CD spectrum, Wolfgang Kabsch for crystallographic advice, and Kenneth C. Holmes for continued support.

REFERENCES

Alber, T. (1989) *Annu. Rev. Biochem. 58*, 765–798.
Anderson, M. W., Reynolds, S. H., You, M., & Maronpot, R. M. (1992) *Environ. Health Perspect.* (in press).
Barbacid, M. (1987) *Annu. Rev. Biochem.* 56, 779–827.
Bollag, G., & McCormick, F. (1991) *Nature 351*, 576–579.
Bos, J. L., Fearon, E. R., Hamilton, S. R., Verlaan-de Vries, M., van Boom, J. H., van der Eb, A. J., & Vogelstein, B. (1987) *Nature 327*, 293–297.
Bourne, H. R., & Stryer, L. (1992) *Nature 358*, 541–543.
Bradford, M. M. (1976) *Anal. Biochem. 72*, 248–254.
Brünger, A. T., Kuriyan, J., & Karplus, M. (1987) *Science 235*, 458–460.
Cambillau, C. (1989) in *Silicon Graphics Geometry Partner Directory* (Silicon Graphics, Ed.) Spring Volume, Mountain View, CA.
Certa, U., Bannwarth, W., Stüber, D., Gentz, R., Lanzer, M., LeGrice, S., Guillot, G., Wendler, I., Hunsmann, G., Bujard, H., & Mous, J. (1986) *EMBO J. 5*, 3051–3956.
Crowther, R. A. (1972) in *The Molecular Replacement Method* (Rossman, M. G., Ed.) pp 173–183, Gordon & Breach, New York.
Downward, J., Graves, J. D., Warne, P. H., Rayter, S., & Cantrell, D. A. (1990) *Nature 346*, 719–723.

Feuerstein, J., Goody, R. S., & Wittinghofer, A. (1987) *J. Biol. Chem. 262*, 8455–8458.
Franks, A. (1955) *Proc. Phys. Soc., London, Sect. B 68*, 1054–1064.
Frech, M., John, J., Pizon, V., Chardin, P., Tavitian, A., Clark, R., McCormick, F., & Wittinghofer, A. (1990) *Science 249*, 169–171.
Gibbs, J. B., Schaber, M. S., Allard, W. J., Sigal, I. S., & Scolnick, E. M. (1988) *Proc. Natl. Acad. Sci. U.S.A. 85*, 5026–5030.
Gideon, P., John, J., Frech, M., Lautwein, A., Clark, R., Scheffler, J. E., & Wittinghofer, A. (1992) *Mol. Cell. Biol. 12*, 2050–2056.
Grand, R. J. A., & Owen, D. (1991) *Biochem. J. 279*, 609–631.
Harada, Y., Lifchitz, A., Berthou, J., & Jolles, P. (1981) *Acta Crystallogr. A37*, 398–406.
Hausser, K. H., & Kalbitzer, H. R. (1991) *NMR in Medicine and Biology. Structure Determination, Tomography, In Vivo Spectroscopy*, Springer-Verlag, Heidelberg.
John, J., Frech, M., & Wittinghofer, A. (1988) *J. Biol. Chem. 263*, 11792–11799.
John, J., Schlichting, I., Schiltz, E., Rösch, P., & Wittinghofer, A. (1989) *J. Biol. Chem. 264*, 13086–13092.
John, J., Sohmen, R., Feuerstein, J., Linke, R., Wittinghofer, A., & Goody, R. S. (1990) *Biochemistry 29*, 6058–6065.
John, J., Rensland, H., Schlichting, I., Vetter, I., Borasio, G. D., Goody, R. S., & Wittinghofer, A. (1993) *J. Biol. Chem.* (in press).
Jones, T. A. (1978) *J. Appl. Crystallogr. 11*, 268–272.
Kabsch, W. (1988a) *J. Appl. Crystallogr. 21*, 67–71.
Kabsch, W. (1988b) *J. Appl. Crystallogr. 21*, 916–924.
Kabsch, W., & Sander, C. (1983) *Biopolymers 22*, 2577–2637.
Krengel, U., Schlichting, I., Scherer, A., Schumann, R., Frech, M., John, J., Kabsch, W., Pai, E. F., & Wittinghofer, A. (1990) *Cell 62*, 539–548.
Matthews, B. W. (1987) *Biochemistry 26*, 6885–6888.
Matthews, B. W., Nicholson, H., & Becktel, W. J. (1987) *Proc. Natl. Acad. Sci. U.S.A. 84*, 6663–6667.
McCormick, F. (1989) *Cell 56*, 5–8.
Milburn, M. V., Tong, L., DeVos, A. M., Brünger, A., Yamaizumi, Z., Nishimura, S., & Kim, S.-H. (1990) *Science 247*, 939–945.
Mistou, M.-Y., Jacquet, E., Poullet, P., Rensland, H., Gideon, P., Schlichting, I., Wittinghofer, A., & Parmeggiani, A. (1992) *EMBO J. 11*, 2391–2397.
Muroya, K., Hattori, S., & Nakamura, S. (1992) *Oncogene 7*, 277–281.
Neal, S. E., Eccleston, J. F., & Webb, M. R. (1990) *Proc. Natl. Acad. Sci. U.S.A. 87*, 3562–3565.
Pai, E., Kabsch, U., Krengel, U., Holmes, K. C., John, J., & Wittinghofer, A. (1989) *Nature 341*, 209–214.
Pai, E. F., Krengel, U., Petsko, G. A., Goody, R. S., Kabsch, W., & Wittinghofer, A. (1990) *EMBO J. 9*, 2351–2359.
Privé, G. G., Milburn, M. V., Tong, L., DeVos, A. M., Yamaizumi, Z., Nishimura, S., & Kim, S.-H. (1992) *Proc. Natl. Acad. Sci. U.S.A. 80*, 3649–3653.
Ramachandran, G. N., Ramakrishnan, C., & Sasisekharan, V. (1963) *J. Mol. Biol. 7*, 95–99.
Read, R. J. (1986) *Acta Crystallogr. A42*, 140–149.
Reinstein, J., Schlichting, I., Frech, M., Goody, R. S., & Wittinghofer, A. (1991) *J. Biol. Chem. 266*, 17700–17706.
Rensland, H., Lautwein, A., Wittinghofer, A., & Goody, R. S. (1991) *Biochemistry 30*, 11181–11185.
Rösch, P., Kalbitzer, H. R., & Goody, R. S. (1980) *FEBS Lett. 121*, 211–214.
Sambrock, J., Fritsch, E. F., & Maniatis, T. (1989) *Molecular Cloning, A Laboratory Manual*, Cold Spring Harbor Laboratory Press, Cold Spring Harbor, NY.
Satoh, T., Endo, M., Nakafuku, M., Akiyama, T., Yamamoto, T., & Kaziro, Y. (1990a) *Proc. Natl. Acad. Sci. U.S.A. 87*, 7926–7929.
Satoh, T., Endo, M., Nakafuku, M., Nakamura, S., & Kaziro, Y. (1990b) *Proc. Natl. Acad. Sci. U.S.A. 87*, 5993–5997.
Scheidig, A., Pai, E. F., Schlichting, I., Corrie, J. E. T., Reid, G. P., Wittinghofer, A., & Goody, R. S. (1992) *Philos. Trans. R. Soc. London, Ser. A 340*, 263–272.
Scherer, A., John, J., Linke, R., Goody, R. S., Wittinghofer, A., Pai, E. F., & Holmes, K. C. (1989) *J. Mol. Biol. 206*, 257–259.
Schlichting, I., Rapp, G., John, J., Wittinghofer, A., Pai, E. F., & Goody, R. S. (1989) *Proc. Natl. Acad. Sci. U.S.A. 86*, 7687–7690.
Seeburg, P. H., Colby, W. W., Capon, D. J., Goeddel, D. V., & Levinson, A. K. (1984) *Nature* 304, 71–75.
Shortle, D. (1989) *J. Biol. Chem. 264*, 5315–5318.
Tanaka, N. (1977) *Acta Crystallogr. A33*, 191–193.
Trahey, M., & McCormick, F. (1987) *Science 238*, 542–545.
Tran-Dinh, S., & Roux, M. (1977) *Eur. J. Biochem. 76*, 245–249.
Tucker, J., Sczakiel, G., Feuerstein, J., John, J., Goody, R. S., & Wittinghofer, A. (1986) *EMBO J. 5*, 1351–1358.
Vogel, U., Dixon, R. A. F., Schaber, M. D., Diehl, R. E., Marshall, M. S., Scolnick, E. M., Sigal, I. S., & Gibbs, J. B. (1988) *Nature 335*, 90–93.
Yount, R. (1975) *Adv. Enzymol. Relat. Areas Mol. Biol. 43*, 1–56.